[Frontiers in Bioscience E3, 489-505, January 1, 2011]

Global analysis of autocorrelation functions and photon counting distributions

Victor V. Skakun[1], Ruchira Engel[2], Anatoli V. Digris[1], Jan Willem Borst[3], Antonie J.W.G. Visser[3]

[1]Deparment of Systems Analysis, Belarusian State University, Minsk, 220050, Belarus,[2]Institute of Membrane and Systems Biology, University of Leeds, Leeds LS2 9JT, United Kingdom, [3]Laboratory of Biochemistry, Microspectroscopy Centre, Wageningen University, 6703 HA Wageningen, The Netherlands

TABLE OF CONTENTS

1. ABSTRACT

In fluorescence correlation spectroscopy (FCS) and photon counting histogram (PCH) analysis the same experimental fluorescence intensity fluctuations are used, but each analytical method focuses on a different property of the signal. The time-dependent decay of the correlation of fluorescence fluctuations is measured in FCS yielding, for instance, molecular diffusion coefficients. The amplitude distribution of these fluctuations is calculated by PCH yielding the molecular brightness. Both FCS and PCH give information about the molecular concentration. Here we describe a global analysis protocol that simultaneously recovers relevant and common parameters in model functions of FCS and PCH from a single fluorescence fluctuation trace. The global analysis approach is described and tested with experimental fluorescence fluctuation data of enhanced green-fluorescent protein (eGFP) and dimeric eGFP (two eGFP molecules connected by a six amino acid long linker) in aqueous buffer. Brightness values and diffusion constants are recovered with good precision elucidating novel excited-state and motional properties of both proteins.

2. INTRODUCTION

In the last decades fluorescence correlation spectroscopy, originally introduced by Elson *et al.* (1-3) in the early 1970s, has become a widely used technique for studying various dynamic molecular processes (see many accounts in the 1990s (4-10)). It has found applications in measuring local concentrations, mobility coefficients, reaction rates and detection of intermolecular interactions *in vitro* and *in vivo,* excellently reviewed in this century(11-17). The sensitivity and non-invasive nature of this technique has made it one of the important techniques for studying molecular processes in cells and thus a useful tool for biochemists, biophysicists and biologists.

Fluorescence fluctuation methods are based on the detection of tiny, spontaneous fluctuations in fluorescence intensity caused due to deviations from thermal equilibrium in an open system. These fluctuations can arise e.g. due to diffusion of fluorescent molecules in and out of a well-defined observation volume generated by a focused laser beam. The intensity fluctuations can be monitored and autocorrelated over time as in fluorescence

correlation spectroscopy (FCS) (13) or a distribution of fluorescence intensity amplitudes can be analyzed as in photon counting histogram (PCH) (18-22) or in fluorescence intensity distribution analysis (FIDA) (23-27).

Over time several developments in fluorescence fluctuation spectroscopy have taken place. Fluorescence cross- correlation spectroscopy (FCCS), reviewed in (13), is an established technique to monitor intracellular protein-protein interaction involving different measuring strategies (one-photon and two-photon excitation with dual-color detection, dual-color one-photon excitation and dual-color detection) (see, for instance, references (28-34)). Dual-color PCH analysis has been developed (35, 36) as well as 2D-FIDA (24, 25). Many technical improvements have been implemented in fluorescence fluctuation spectroscopy. Dual-focus FCS has been developed to remove experimental artifacts (37-39). Novel excitation strategies have been designed such as alternating laser excitation (40) or pulsed interleaved excitation (41) to remove cross-talk in dual channel measurements and modulated excitation to suppress triplet state buildup while keeping complete time range information in FCS (42). Fluorescence lifetime correlation spectroscopy has been developed to observe single dye diffusion in two distinct environments (43, 44). Scanning FCS has been implemented for precise measurements of diffusion coefficients (45). Total internal reflection FCS has been utilized to measure diffusion processes in the small confines of an evanescent field (46-49). Large progress has been made in the field of image correlation spectroscopy (reviewed by Kolin and Wiseman in 2007 (50)) and raster scanning image correlation spectroscopy (51-53).

Performing fluorescence fluctuation spectroscopy (FFS) experiments is relatively straightforward. But the theory for FFS is based on several assumptions, which do not always hold in a real experimental situation. For example, FFS analysis assumes that the experimental observation volume is Gaussian, which is not always true especially for *in vivo* measurements (54). Dead time and afterpulsing of the photodetectors may influence PCH analysis (55). There are a number of optical factors that influence FFS measurements such as cover-slide thickness, refractive index of the sample and optical saturation that should be taken into account for proper analysis (56, 57). In a confocal configuration for one-photon excitation a PCH model with a three-dimensional Gaussian observation volume profile does not adequately fit the experimental fluorescence fluctuation data (58, 59). In addition, there is a clear effect of bin time on PCH analysis, which influences the estimation of molecular concentration and brightness (25, 60). While it is crucial that the experimental setup must be optimized to close to ideal conditions, one should also be aware of all these factors in the data analysis procedure to avoid erroneous fits and misinterpretation of the experimental data.

We have previously described the FCS data processor, which can be used to analyze FCS data (61). The FCS data processor provides the user with the flexibility of using different models and rigorous error analysis to judge the quality of the fit and decide on the model that best describes the data. By allowing the user to generate initial guesses, link and constrain fit parameters and fit several autocorrelation function (ACF) curves globally, it also improves the accuracy and speed of analysis. However, since both FCS and PCH/FIDA use the same experimental data it is lucrative to be able to analyze one set of data to get all the information about dynamics and brightness of the molecular species.

Here we describe new data analysis software, the FFS data processor that allows the complete analysis of FFS data. It incorporates all the features of the FCS data processor with additional possibilities of performing FIDA and PCH analyses on the experimental photon counting distributions (PCD). Starting from the recorded flow of photon arrival times (raw data) the FFS data processor allows the users to generate an ACF, PCD or other statistical characteristics of photon flows such as factorial cumulants (62). Several photon-counting distributions, generated at different bin times, can be analyzed globally to give robust values for the molecular brightness (25). It is also possible to perform global analyses of PCDs and ACFs simultaneously resulting in more accurate values of triplet-state and diffusion parameters, and also in robust, time-independent estimations of molecular brightness and number of molecules. The FFS data processor also implements various corrections for differences in shapes of confocal volumes, background fluorescence and for dynamic processes in intensity distribution analyses. The use of the software is demonstrated through fitting of experimental fluorescence fluctuation data obtained from monomeric and dimeric forms of enhanced green-fluorescent protein (eGFP) in aqueous buffer.

3. REVIEW OF THEORY

3.1. Fluorescence intensity distribution analysis

The theory of FIDA is based on the use of generation function (GF) concept. The photon counting generating function of the probability $P(n)$ of detecting n photons emitted by a number of fluorescent molecules in a system at equilibrium in an open non-homogeneous observation volume V during a counting time interval (bin time) T can be written as (23):

$$G(\xi) = \exp\left(\lambda T(\xi - 1) + \sum_i C_i \int_V \left(e^{(\xi-1) q_i T B(\mathbf{r})} - 1 \right) d\mathbf{r} \right), \quad (1)$$

where i is an index of molecular species, C_i is the concentration, q_i is the specific brightness of molecules (in counts per second per molecule), $B(\mathbf{r})$ is the brightness profile function, which is the product of excitation intensity and detection efficiency**,** and λ is the mean background count rate of the detector. Brightness q is defined as $q = I_0 \sigma_a Q \kappa$, where I_0 is the excitation intensity in the focus, σ_a ..... fluorescence quantum yield, respectively, and κ is the detection efficiency of the confocal setup. It is assumed that the contribution of each single molecule to

the recorded photon trace is independent and the emission intensity is constant during the counting time interval *T*.

Having the GF, it is easy to calculate the photon counting distribution, *P*(*n*), using inverse Fast Fourier Transform (FFT) of the characteristic function, which can be obtained from the GF by substituting ξ by the complex exponent $e^{i\varphi}$ (23):

$$P(n) = FFT^{-1}(G(e^{i\varphi})),\ n = 0,1,\ldots,m-1,\ \varphi = 2\pi n/m, \quad (2)$$

where *m* is the number of data points in the PCD.

The key advantage of the FIDA lies in the flexibility of a polynomial model for the brightness profile function allowing an approximation for a broad spectrum of confocal volume shapes (23, 25):

$$d\mathbf{r}/dx = A_0\,(x + a_1x^2 + a_2x^3),\ x = \ln\left[B_0/B(\mathbf{r})\right], \quad (3)$$

where a_1, a_2 are adjustable instrumental parameters. A_0 is the volume scaling parameter and B_0 is the brightness in the focus. B_0 and A_0 can be calculated from normalization equations:

$$\chi_1 = \int_V B(\mathbf{r})d\mathbf{r}, \quad \chi_2 = \int_V B^2(\mathbf{r})d\mathbf{r}. \quad (4)$$

Substituting Eq. 3 into Eqs. 4 gives:

$$\begin{aligned} A_0' &= \chi_1^2\,(2a_1 + 3a_2 + 2)/[8\chi_2(2a_1 + 6a_2 + 1)^2], \\ B_0' &= 8\chi_2(2a_1 + 6a_2 + 1)/[\chi_1(2a_1 + 3a_2 + 2)]. \end{aligned} \quad (5)$$

Finally, one obtains:

$$G(\xi) = \exp\left(\lambda T(\xi - 1) + A_0\sum_i N_{FIDA\,i}\int_0^\infty\left(\exp\left[(\xi - 1)B_0q_{FIDA\,i}Te^{-x}\right] - 1\right)\left(x + a_1x^2 + a_2x^3\right)dx\right), \quad (6)$$

where

$$A_0 = (2a_1 + 3a_2 + 2)/[8(2a_1 + 6a_2 + 1)^2],$$
$$B_0 = 8(2a_1 + 6a_2 + 1)/(2a_1 + 3a_2 + 2) \text{ and}$$
$$N_{FIDA\,i} = C_i\,\chi_1^2/\chi_2,\ q_{FIDA\,i} = q_i\chi_2/\chi_1. \quad (7)$$

3. 2. Photon counting histogram analysis

In PCH the total PCD from a number of molecules is calculated by successive convolutions of single-molecule PCDs (18):

$$p^{(1)}(n,q) = \frac{1}{QV_{eff}}\int_{-\infty}^{\infty} Poi(n, qTB(\mathbf{r}))d\mathbf{r}, \quad (8)$$

where $p^{(1)}(n,q)$ is a single-molecule PCD, $Poi(n, \eta)$ denotes the Poisson distribution with the mean value η, $B(\mathbf{r})$ is assumed to be Gaussian and *Q* is a constant taken such that the product QV_{eff} is large enough to completely include the illuminated volume. The distribution *P*(*n*) of a number of molecules N_{eff} in an open effective observation volume $V_{eff} = \chi_1^2/\chi_2$ is the weighted average of $p^{(1)}(n,q)$ convolved *M* times (18):

$$\begin{aligned} &P(n, N_{eff}, q) = \sum_{M=0}^{\infty} p^{(M)}(n,q)\,Poi(M, QN_{eff}), \\ &p^{(M)}(n,q) = \underbrace{p^{(1)} \otimes \ldots \otimes p^{(1)}}_{M\ times}(n,q),\ p^{(0)}(n,q) = \begin{cases} 1, n = 0, \\ 0, n \neq 0. \end{cases} \end{aligned} \quad (9)$$

Finally, the PCD of a number of independent species is given by a convolution of the PCD of each species

$$P(n) = P(n, N_{eff\,1}, q_1) \otimes \ldots \otimes P(n, N_{eff\,n}, q_n). \quad (10)$$

Correction for the background can be applied to PCH similarly as it is done in FIDA (23). Since the background signal has Poissonian statistics, it can be accounted for by an additional convolution with Poisson distribution with parameter λT

$$P(n, \lambda) = P(n) \otimes Poi(n, \lambda T). \quad (11)$$

Eqs. 8-9 often fail to fit one-photon excitation experimental data due to the large deviation of an actual brightness profile from an assumed 3D Gaussian approximation (23, 59). To improve the model, Perroud *et al.* (58) and Huang *et al.* (59) introduced additional fitting parameters F_k defined as the relative difference between the integral χ_k of the k^{th} power of the actual brightness profile function $B(\mathbf{r})$ (normalized to unity) and that of its 3D Gaussian approximation χ_{Gk}.

$$F_k = (\chi_k - \chi_{Gk})/\chi_{Gk}. \quad (12)$$

Introducing F_k (Eq. 12) into the single-molecule PCD (Eq. 8) leads to (59, 63):

$$p^{(1)}(n, q_C) = \frac{1 + F_2}{(1 + F_1)^2}\left[p_G^{(1)}(n, q_C) + \frac{1}{n!Q}\sum_{k=n}^{\infty}\frac{(-1)^{k-n}(q_CT)^kF_k}{(k-n)!(2k)^{3/2}}\right], \quad (13)$$

where $p_G^{(1)}(n, q_C) = \int_{-\infty}^{\infty} Poi(n, q_CTB_G(\mathbf{r}))d\mathbf{r}/QV_{eff}$ and q_C is equal to:

$$q_C = (1 + F_1)q/(1 + F_2). \quad (14)$$

In most cases only the first-order correction (all F_k equal to zero except F_1) is sufficient to get the best fit to the experimental data.

The polynomial approximation (Eq. 3) of the observation profile can be also applied to the PCH model. Eqs. 8 and 9 then take the form:

$$\begin{aligned} &p^{(1)}(n, q_{FIDA}) = \frac{A_0}{Q}\int_0^{\infty} Poi(n, q_{FIDA}TB_0e^{-x})(x + a_1x^2 + a_2x^3)dx, \\ &P(n, N_{eff}, q_{FIDA}) = \sum_{M=0}^{\infty} p^{(M)}(n, q_{FIDA})\,Poi(M, QN_{FIDA}) \end{aligned} \quad (15)$$

In this definition, results of PCH analysis with a polynomial profile are fully equivalent to results of FIDA.

3.3. Fluorescence correlation spectroscopy

The autocorrelation function describing j independent molecular species diffusing freely in a 3D-Gaussian shaped observation volume is (61):

$$G(t) = G_{\inf} + \frac{1 - F_{trip} + F_{trip} e^{-t/\tau_{trip}}}{(1 - F_{trip})\left(\sum q_j N_{eff\,j}\right)^2} \sum_i \frac{q_i^2 N_{eff\,i}}{\left(1 + \frac{t}{\tau_{diff\,i}}\right)\sqrt{\left(1 + \frac{t}{a^2 \tau_{diff\,i}}\right)}}, \quad (16)$$

where $G_{\inf} = G(\infty)$, F_{trip} and τ_{trip} are, respectively, the fraction and the relaxation time of molecules in the triplet state, $a = \omega_z / \omega_{xy}$, ω_{xy} and ω_z are, respectively, the lateral and axial radii of the confocal detection volume, and τ_{diff} is the lateral diffusion time, which is related to the diffusion coefficient D_{tran} via $\tau_{dif} = \omega_{xy}^2/(4D_{tran})$. In Eq. 16 it is assumed that each molecular species has the same triplet-state characteristics. For more details see comprehensive reviews (13, 16, 17).

3.4. Correction for dynamic processes in photon counting distribution analysis

Eqs. 1, 6, 8, 13 and 15 were derived under the assumption that the fluorescence intensity emitted by a molecule during bin time T is constant, which is valid for the limit of short bin times. The theory for an arbitrary bin time T was developed and successfully applied for analysis of PCDs (25, 26, 60, 64, 65). The most practical way to account for diffusion and other processes like triplet-state relaxation is to correct the brightness and number of molecules such that the first and second factorial cumulants of the PCD are exact (25, 60). It is just an approximation, because only the first two cumulants of PCD are exact, but it works well for a relatively wide range of experimental conditions (64). According to this theory one has to calculate the so-called binning correction factor (25, 60):

$$B_2(T) = \frac{2}{T^2}\int_0^T (T - t) g(t) dt \,, \quad (17)$$

where $g(t)$ is a time dependent term of autocorrelation function in FCS

$$g(t) = \frac{1 - F_{trip} + F_{trip} e^{-t/\tau_{trip}}}{1 - F_{trip}} \frac{1}{\left(1 + \frac{t}{\tau_{diff}}\right)\sqrt{\left(1 + \frac{t}{a^2 \tau_{diff}}\right)}} \quad (18)$$

and to correct the brightness and the number of molecules in the following form:

$$\begin{aligned} q_0 &= q(T)/B_2(T), \\ N_0 &= N(T) B_2(T), \end{aligned} \quad (19)$$

where $q(T)$ and $N(T)$ are apparent parameters of the model dependent on bin time T and q_0 and N_0 are absolute values of brightness and concentration that are independent of T. In general, the binning correction factor can be calculated assuming two or even more diffusing components (such correction can be applied to a mixture of species with approximately equal brightness values but quite different hydrodynamic radii). For a model of multiple brightness components this correction has to be applied independently to each component. Triplet and diffusion characteristics can be either different or the same for each brightness component.

3.5. Relation between number of molecules and brightness in FCS, PCH and FIDA

The reference volume in PCH and FCS is defined as $V_{eff} = \chi_1^2/\chi_2$. The same definition of the reference volume is implicitly obtained in FIDA as can be seen from Eq. 7 and $V_{FIDA} = \chi_1^2/\chi_2 = V_{eff}$. Thus, the number of molecules $N_{FIDA} = N_{eff}$. However, $q_{FIDA} = q\chi_2/\chi_1 = \gamma_2 q$, where $\gamma_2 = \chi_2/\chi_1$. Correction of the brightness profile through Eq. 12 also influences the value of the brightness (see Eq. 14). Thus, neither FIDA nor PCH with brightness profile correction returns the true brightness q. The following relations must be taken into account (63):

$$q_{FIDA} = \gamma_2 q \,,\; q_C = (1 + F_1) q / (1 + F_2) \,. \quad (20)$$

For the sake of simplicity in the equations we have omitted the subscript 0 because these equations are valid for both q_0, N_0 and $q(T)$ and $N(T)$. While performing FCS and PCH/FIDA on the same data one usually likes to relate brightness calculated from the average intensity $<I>$ to the brightness obtained from PCH/FIDA. In FIDA the expression for the first factorial cumulant K_1 takes the following form (25):

$$K_1 = \lambda T + \sum_i N_{0\,FIDA\,i} q_{0\,FIDA\,i} T \,. \quad (21)$$

Similarly, for PCH analysis with brightness profile correction one obtains:

$$K_1 = \lambda T + \gamma_2 \frac{(1 + F_2)}{(1 + F_1)} \sum_i N_{0\,eff\,i} q_{0\,C\,i} T \,. \quad (22)$$

Thus:

$$< I >= \frac{K_1}{T} = \lambda + \sum_i N_{0\,FIDA\,i} q_{0\,FIDA\,i} = \lambda + \gamma_2 \frac{(1 + F_2)}{(1 + F_1)} \sum_i N_{0\,eff\,i} q_{0\,C\,i}$$

.

For a one-component model without background one obtains:

$$< I >= N_{0\,FIDA} q_{0\,FIDA} = \gamma_2 (1 + F_2) N_{0\,eff} q_{0\,C} / (1 + F_1) \,. \quad (23)$$

Since the number of molecules in FCS does not depend on time, N_{FCS} is equal to N_{0eff} and

$$q_{FCS} = < I > / N_{0\,eff} = q_{0\,FIDA} = \gamma_2 (1 + F_2) q_{0\,C} / (1 + F_1) \,. \quad (24)$$

3.6. Weighting of autocorrelation- and photon counting distribution functions

Weighting factors (66) of the ACF are calculated by the algorithm proposed by Wohland *et al.* (67). The intensity trace is subdivided into a number of non-

overlapping sub-traces and the local autocorrelation function is calculated from each sub-trace. Then standard deviations for each point of the ACF are obtained from these local autocorrelation functions. Finally weighting factors of the ACF are calculated by dividing the obtained deviations by the square root of the number of sub-traces. This algorithm does not depend on the type of the ACF time scale (quasi-logarithmic or linear) and FCS model parameters (i.e. it does not require any prior knowledge about the explored system) and usually results in good estimations of standard deviations of the ACF. Weighting factors of the PCD are calculated as standard deviations of binomial distribution given by $\sigma_i = \sqrt{mp_i(1-p_i)}$, where m is the total number of bins and $p_i = P^*(i)$ (* denotes the experimental PCD). Because m is usually large, a binomial distribution is well approximated by a normal distribution and therefore the application of reduced χ^2 criterion is justified.

4. MATERIALS AND METHODS

4.1. Samples

Monomeric and dimeric eGFP were purified according to a recently described procedure (68). The two eGFP molecules in the dimer were linked by six amino acids (GSGSGS). Purified monomeric and dimeric eGFP solutions were in 50 mM TRIS buffer (pH 8.0). For the measurements 200-µl solutions were added to an 8-chambered coverglass (Lab-Tek, Nalge Nunc International Corp., USA). Rhodamine 110 (R110) (Invitrogen, Breda, The Netherlands) in water was used for calibration measurements.

4.2. Instrumentation

The measurements were performed on the ConfoCor 2 - LSM 510 combination setup (Carl Zeiss, Jena, Germany) detailed in (31, 69, 70). eGFP was excited with the 488 nm line from an argon-ion laser (excitation intensity in the range 10-40 µW) focused into the sample with a water immersion C-Apochromat 40x objective lens N.A. 1.2 (Zeiss). After passing through the main beam splitters HFT 488/633 the fluorescence was filtered with a band pass 505-550. The pinhole for confocal detection was set at 70 µm. The microscope was controlled by Zeiss AIM 3.2 software. Raw intensity fluctuation data consisting of up to 4 x 10^6 photons were collected from single measurements. The data collection time ranged between 30 s and 120 s.

5. RESULTS AND DISCUSSION

5. 1. General comments on global analysis

Dependence of model parameters in PCH on the bin time makes it difficult to recover the true time-independent brightness and number of molecules from just a single photon counting distribution. An attempt to fit PCD calculated at a very small bin time to avoid any influence of diffusion and triplet kinetics usually fails if the photon count rate is not high enough. The PCD calculated at such conditions has only a few data points, which makes it difficult to fit the data well. To get time-independent brightness and number of molecules from a fit of PCD calculated at higher bin time, knowledge of diffusion and triplet parameters is required (see Eqs. 17-19). FCS has been established as a robust method for estimation of triplet and diffusion parameters (71). Therefore it is advantageous to combine the features of both complementary FFS methods and to increase the information content available from a single measurement.

The fit of a set of PCDs calculated at different bin times in fluorescence intensity multiple distribution analysis (FIMDA) (25) or photon counting multiple histograms (PCMH) (60) allows recovering all parameters (including triplet and diffusion parameters) from a single analysis. However, both FIMDA and PCMH have a drawback. These methods use the correction in the form of an integral (see Eq. 17). It means that the same correction value $B_2(T)$ can be achieved for a different functional form of $g(t)$; for example, one can set diffusion time to a very small value and compensate this by an appropriate triplet fraction and decay parameter values, and *vice versa*. Therefore after global analysis of several PCDs the fit can be satisfactory but results in erroneous values for diffusion, triplet and also for other parameters because of the presence of many local minima in the multi-dimensional space of fit parameters. As a consequence, the recovered parameters usually have much wider confidence intervals compared to those obtained by traditional FCS analysis.

Although good results can be obtained from a two-step analysis (fit of the ACF followed by a fit of the PCD while fixing diffusion and triplet parameters to values obtained in the first step), better results can be expected from global analysis of both ACF and PCD. Only one run of the fit is required to get estimations for all fit parameters in this case. The number of molecules appears in both FCS and PCH models and can be linked together. It already makes the global analysis of ACF and PCD more advantageous in comparison to a two-step analysis, because it allows reducing the number of fit parameters by one while increasing the total number of data points available for the analysis. The structure parameter, diffusion and triplet parameters in the FCS model and in the part correcting for triplet and diffusion kinetics in the PCH/FIDA model can also be linked together. Consequently, FCS will provide accurate and robust estimations for triplet and diffusion parameters thus minimizing the risk of obtaining erroneous parameter values. *Vice versa* PCH/FIDA will yield correct time-independent estimations for the brightness that helps to obtain correct concentrations in FCS, if the sample contains two (or more) brightness components (see Eq. 16). Factors γ_2 and $(1+F_1)/(1+F_2)$ presented in the relation of q_{FIDA} and q_C with the true brightness (see Eq. 20) are independent of the number of components. It allows the use of global analysis of PCH, FIDA and FCS in any combination. In contrast to FIMDA and PCMH, global analysis of ACF and PCD allows extraction of time-independent values for brightness and concentration for molecular samples using just a single PCD and a single ACF. However, taking into account that PCD usually has a low number of data points,

it is advisable to calculate several PCDs to increase the brightness information content of experimental data.

One advantage of FCS lies in its insensitivity to the emission of molecules that are outside the focal point of the laser excitation beam along the optical axis (out-of-focus emission). The signal from these molecules is averaged in the calculation of the autocorrelation function and its contribution successfully canceled due to the chosen normalization. However, it is not true for PCH analysis and FIDA. The photon counting distribution keeps the information about each detected photon. It was shown (59, 60) that the first-order profile correction in PCH directly accounts for the out-of-focus emission. Taking into account the fact that PCH/FIDA is not sensitive to the difference in ω_{xy} and ω_z in contrast to FCS (59) one can conclude that the out-of-focus emission rather than the shape of the brightness profile itself has to be taken into account when performing global analysis of PCD and ACF.

5.2. Modification of the global χ^2 criterion

Global analysis of experimental data obeying different functional forms may result in overestimation (or underestimation) of some model parameters, if appropriate weighting factors are not applied to each data point. This is especially important when the number of data points in these functions is quite different, for instance the ACF usually has 175 experimental data points *versus* only 15 data points in PCD. Such difference in number of data points leads to a significant difference in the number of degrees of freedom (calculated as number of data points minus number of fit parameters minus one) corresponding to each analyzed curve. Thus, the standard global χ^2 criterion (72) becomes relatively insensitive to small deviations between the analyzed and best fit curves, for the curves with the lower degrees of freedom. To avoid this problem a modified χ^2 criterion is proposed that takes into account the specific weight of each individual curve that participates in the global analysis. The equation of this modified χ^2 is the following:

$$\chi^2_{gl\,\mathrm{mod}} = \frac{N-m-M}{M(N-m+\sum_{i=1}^{M} m_i^{lnk} - m^{gr} - 1)} \sum_{i=1}^{M} \left(\frac{1}{n_i - m_i - 1} \sum_{j=1}^{n_i} \frac{\left(x_{ij} - F_{ij}^{th}\right)^2}{\sigma_{ij}^2} \right), \quad (25)$$

where x_{ij} and σ_{ij} are the measured value and the standard deviation of the i^{th} experimental data point in the j^{th} measured curve and F_{ij}^{th} is the theoretical value for this point; M is the number of globally analyzed curves; n_i is the number of points in i^{th} curve ; m_i and m_i^{lnk} is the number of free and linked parameters in i^{th} model respectively, m^{gr} is the number of parameter groups (sets of linked parameters), $N = \sum_{i=1}^{M} n_i$, $m = \sum_{i=1}^{M} m_i$. As follows from Eq. 25 the contribution of each analyzed curve to the value of the global χ^2 is made equal by dividing the sum in brackets by the corresponding number of degrees of freedom (thus obtaining the local χ^2) and finally multiplying the total sum of the local χ^2 by the average number of degrees of freedom $\left(N-m-M\right)/M = \sum_{i=1}^{M}\left(n_i - m_i - 1\right)/M$. In case of equal number of degrees of freedom in each model ($n_1 = \ldots = n_M$; $m_1 = \ldots = m_M$) Eq. 25 reduces correctly to the standard global χ^2 criterion (72):

$$\chi^2_{gl} = \frac{1}{(N-m+\sum_{i=1}^{M} m_i^{lnk} - m^{gr} - 1)} \sum_{i=1}^{M} \sum_{j=1}^{n_i} \frac{\left(x_{ij} - F_{ij}^{th}\right)^2}{\sigma_{ij}^2} . \quad (26)$$

5.3. Monomeric and dimeric eGFPs as an experimental test system

Analysis of fluctuating fluorescence intensity data of monomeric eGFP has been performed in the FFS data processor by global analysis of one ACF and two PCD's calculated from raw data with bin times of 50 μs and 100 μs, respectively, linking all common parameters. The FCS model with brightness correction (Eq. 16) and the PCH model with second-order corrected Gaussian profile (Eqs. 9-11, 13; k = 1, 2) and triplet-diffusion correction (Eqs. 17-19) were used in the analysis. A complete algorithm of the PCH model calculation is presented in Figure 1. Steps, needed for calculation of a single-component PCH, are presented. For a two-component PCH one needs to perform these steps independently for each component and then to convolve the obtained arrays (Eq. 10).

At the beginning of the analysis only the ACF was fitted in order to get proper initial guesses for the parameters F_{trip}, τ_{trip}, τ_{diff} and a. Then PCDs were added to the analysis and parameter groups were formed. The parameters N_{0eff}, F_{trip}, τ_{trip}, τ_{diff} and a were linked across all models (FCS and PCH) and F_1, F_2 and q_{0C} only across the PCH model. The parameter G_{inf} was fixed to unity and the parameter λ was fixed to zero. Performing the preliminary analysis of ACF is advisable, because the FFS data processor does not calculate initial guesses for the correcting parameters F_{trip}, τ_{trip}, τ_{diff} and a of the PCH model (see Eq. 18). Initial guesses for these parameters can not be obtained from a separate PCD. It was found that the global analysis of some PCDs (as well as some PCDs and ACF together) started from non-optimal initial guesses, are often trapped in local minima due to the integral form of the applied correction (see Eq. 17). Therefore, starting the global fit from almost optimal values of F_{trip}, τ_{trip}, τ_{diff}, a prevents the analysis from trapping in local minima and increases its stability.

Global analysis of eGFP monomer data was done either separately or in combination with R110 calibration data. In the latter case parameters F_1, F_2 and a were linked across both sets of data (6 curves in total) while parameters N_{0eff}, F_{trip}, τ_{trip} and τ_{diff} formed two different sets of parameter groups. Analysis, being performed on a typically current personal computer (Intel Core 2 Duo 2GHz, 2Gb RAM), lasted not more than a few seconds in all cases. Confidence intervals at the 67% confidence level were calculated by the asymptotic standard-errors method as described in (73). The true value of the brightness q_0 was calculated via Eq. 20. Analysis results of monomeric eGFP are summarized in Table 1. Graphical results are shown in Figure 2. The last column in Table 1 represents global

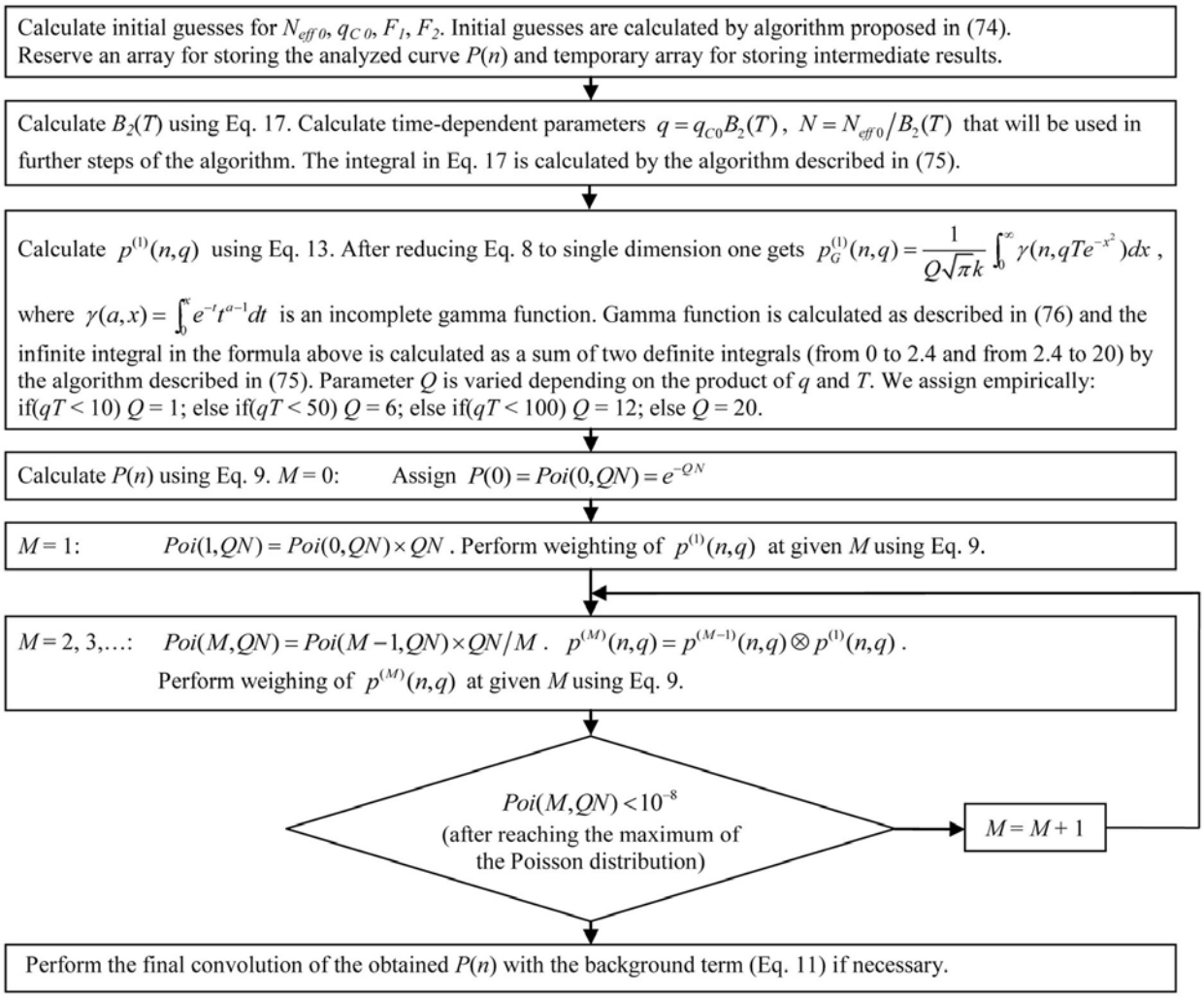

Figure 1. Algorithm of photon counting histogram calculation

analysis results of eGFP and R110 together. Although the recovered parameters are nearly identical in both separate and combined analyses, two PCDs of calibration data were not fitted well in the combined analysis. Local χ^2 criteria were 8.0 and 2.6 in comparison to 3.4 and 1.2 in the analysis of R110 only. It is a consequence of the high sensitivity of the PCH model to the value of correction parameters F_1 and F_2. Therefore it is advisable to link these correction parameters in the global analysis of several measurements only if they do not differ too much. It can be argued that the out-of-focus signal (accounted for by parameters F_1, F_2) shows small variations from measurement to measurement. Although parameters F_1, F_2 are descriptive parameters of the used setup (59), it is not advisable to fix them to any value, as even small deviations of these parameters from the best-fit value will affect the resulted PCD substantially. In contrast to the standard one the modified global χ^2 criterion is sensitive to deviation of any curve from the best fit (see Table 1). We have listed all local χ^2 criterion values in Table 1 to compare standard and modified χ^2 criteria.

Measurements were performed on different days in order to examine whether brightness values can be related to different excitation intensities. Brightness values obtained from the calibration dye R110 enable comparing brightness values of eGFP measured on different days. Taking into account that the brightness value depends on the laser intensity applied to the sample, it can be recalculated accurately enough from one measurement to another (in the non saturated regime) by applying the formula $q_0^{eGFP2} = q_0^{eGFP1} q_0^{calibr2} / q_0^{calibr1}$. We obtained $q_0^{eGFP2} =$ 27422 cpsm (counts per second per molecule), which is very close to the value obtained from the analysis (see Table 1).

We have presented the theory of PCH with Gaussian (Eqs. 9-11, 13; k = 1, 2) and polynomial (Eqs. 10, 11, 15) profiles. Both PCH models as well as the FIDA model can be used in the global analysis together with the model for FCS (Eq. 16). To test the theory and to compare results obtained using either Gaussian or polynomial

Table 1. Results of global analysis of autocorrelation function (ACF) and photon counting distributions (PCDs) of monomeric eGFP and R110 (calibration dye)

Parameter groups	R110 1st day	R110 2nd day	eGFP 1st day	eGFP 2nd day	R110 + eGFP 1st day	
					R110	eGFP
F_1	0.56 ± 0.06	0.55 ± 0.03	0.60 ± 0.06	0.63 ± 0.03	0.63 ± 0.04	
F_2	0.04 ± 0.015	0.046 ± 0.006	0.025 ± 0.015	0.045 ± 0.009	0.042 ±0.01	
a	6.0 ± 0.47	6.0 (fixed)	6.0 (fixed)	6.0 (fixed)	6.0 (fixed)	
F_{trip}	0.16 ± 0.12	0.13 ± 0.10	0.33 ± 0.04	0.21 ± 0.02	0.36 ± 0.12	0.32 ± 0.12
τ_{trip}, µs	1.02 ± 0.85	1.01 ± 0.69	1.68 ± 0.23	2.15 ± 0.25	0.80 ± 0.28	1.74 ± 0.28
τ_{diff}, µs	15.9 ± 0.49	17.3 ± 0.17	71.8 ± 0.49	73.3 ± 0.37	16.1 ±0.27	71.9 ±0.49
N_{0eff}	0.362 ± 0.006	0.363 ± 0.002	2.185 ± 0.008	2.469 ± 0.006	0.365 ± 0.004	2.187 ± 0.008
$q_{0C} \times 10^3$, cpsm	48.9 ± 14.1	61.5 ± 0.85	33.5 ± 0.70	43.0 ± 0.56	50.7 ± 0.97	33.6 ± 0.53
$q_0 \times 10^3$, cpsm	32.69	41.65	21.53	27.53	32.46	21.50
$\chi 2_{gl}$	1.21	1.40	1.27	1.34	1.26	
$\chi 2_{local}$	1.21; 3.36; 1.16	1.46; 2.45; 1.48	1.45; 0.9; 0.72	1.22; 2.05; 1.66	1.2; 8.03; 2.63	1.44; 1.73; 0.85
$\chi 2_{gl\ mod}$	1.742	1.671	0.953	1.34	2.43	

PCD's were calculated with bin times of 50 µs and 100 µs. Data taken on the first day consisted of 2.4×10^5 photons for R110 and 6.5×10^5 photons for eGFP. Data were taken on the second day with four times higher laser intensity and amounted to 1×10^6 photons for R110 and 4×10^6 photons for eGFP. Both χ^2 global criteria (standard and modified) are presented for comparison. Local χ^2 criteria are listed in the following order: ACF, PCD_1, PCD_2

profiles we performed an analysis of fluorescence fluctuations from monomeric eGFP and dimeric eGFP. The PCH model with the polynomial profile was calculated by the algorithm shown in Figure 1 with some modifications. The initial guesses were generated assuming a polynomial approximation, Eq. 15 was used instead of Eq. 8. The upper integration limit in Eq. 15 was set to 50 and different values of Q were assigned (if($qT < 10$) $Q = 1$, else if($qT < 5$) $Q = 6$, else if($qT < 50$) $Q = 5$, else $Q = 40$). Measurements were performed directly after each other to avoid artifacts related to different experimental conditions. Graphical results are shown in Figure 3. Recovered parameters and χ^2 criteria values are summarized in Table 2. After inspection of the results we can conclude that PCH analyses with both brightness profile approximations fit the experimental data equally well. Parameter values and theoretical curves are nearly identical and indistinguishable proving that both approximations can be used in the global analysis. Therefore these approximations can be used together in the global analysis. The pathways to reach global minima (and therefore intermediate fit parameter values) can differ, but the final result does not depend much on the used approximation.

Inspection of a large number of analyzed data showed that PCH analysis with a polynomial profile gave better results than PCH analysis with a Gaussian-corrected profile. In some cases good results could only obtained using PCH analysis with a polynomial profile. On the other hand, application of PCH analysis with a Gaussian profile is advantageous in a number of cases, because the best fit is obtained just by using a first-order correction. This drastically minimizes the risk of overfitting the data. It is therefore advisable to first try the PCH analysis with a Gaussian profile. When the obtained fit results are not acceptable, PCH analysis with a polynomial profile should be applied.

Finally, to compare these results with those available from fits of multiple PCDs calculated at different bin times, two additional analyses using FIMDA and PCMH approaches were performed. We selected measurements of monomeric eGFP that were obtained on the first day (see Table 1). Thirty PCD curves were globally (FIMDA) or sequentially (PCMH) analyzed and results are collected in Table 3 (graphical results are not shown). Although there is close agreement between most recovered parameters, unrealistic estimations were obtained for the triplet-state parameters. Confidence intervals of triplet and diffusion parameters are also wider as compared to global analysis of one ACF and two PCDs despite analysis of only three curves in the latter case.

5.4. Comparison of brightness values and diffusion times of monomeric and dimeric eGFPs

Since we have obtained brightness values and diffusion times with good precision, the recovered parameters for monomeric and dimeric eGFPs can be closely compared. The brightness values (q_0) are 34480 cpsm for monomeric eGFP and 59340 cpsm for dimeric eGFP (Table 2). The ratio of the values $q_0^{\text{dimer}} / q_0^{\text{monomer}} = 1.72$. Thus, the brightness of the eGFP-dimer is less than twice that of the eGFP-monomer. This can be explained by the presence of resonance energy transfer in dimeric eGFP. It must be noted that the two eGFP molecules are linked together by only six amino acids. One of the excited eGFP molecules transfers energy to the other eGFP molecule in the ground state, but does this with less than 100% efficiency. This is demonstrated by time-resolved fluorescence anisotropy experiments, which will be published separately.

The diffusion times (τ_{diff}) are 62.4 µs for monomeric eGFP and 95.1 µs for dimeric eGFP. The ratio of diffusion times is the inverse of the ratio of translation diffusion constants, therefore $\tau_{diff}^{\text{monomer}} / \tau_{diff}^{\text{dimer}} = D_{\text{dimer}} / D_{\text{monomer}} = 0.656$. eGFP-monomer has a molecular mass of 27 kDa and eGFP-dimer has twice this mass, 54 kDa. When we assume that both proteins have a spherical shape, then

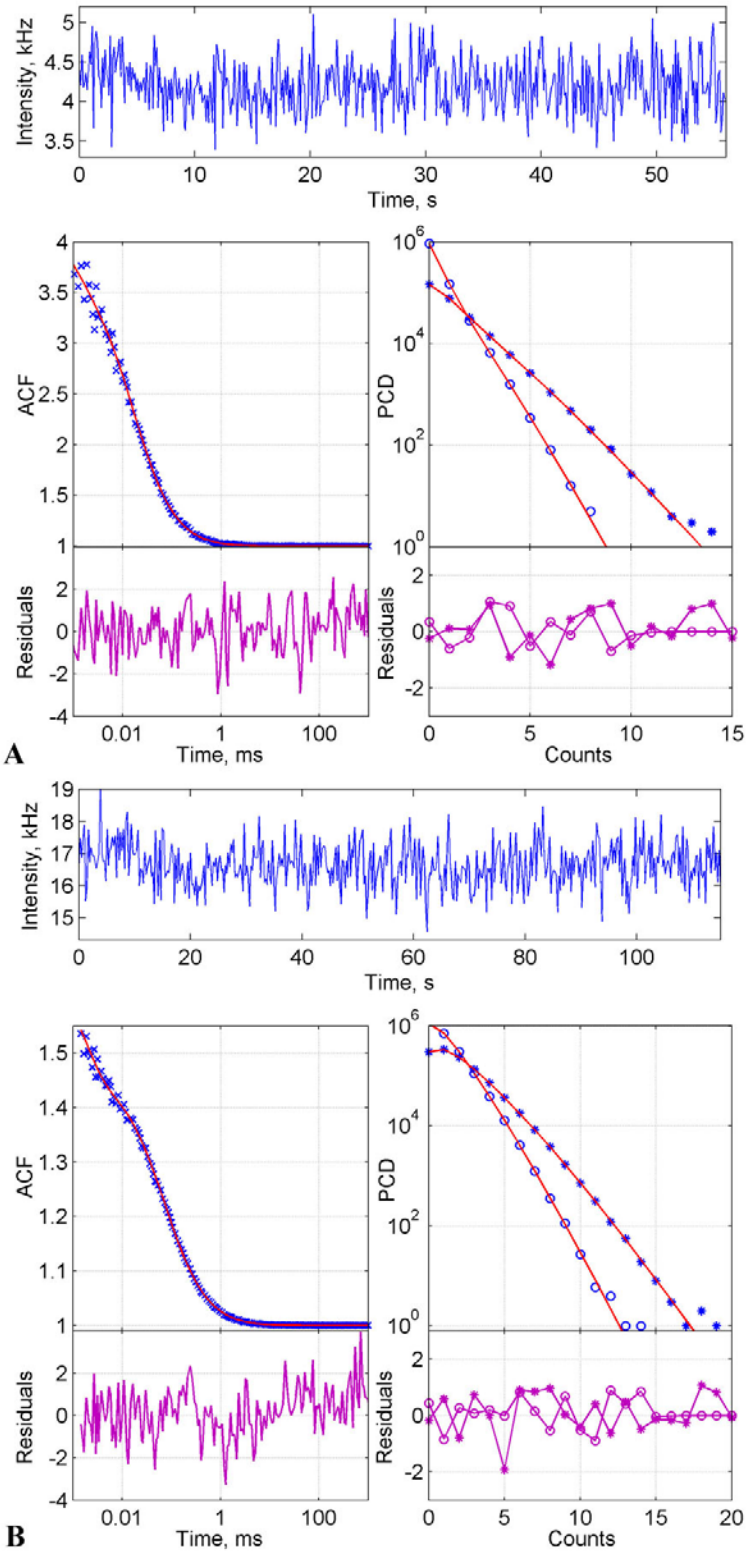

Figure 2. Results of global analysis of autocorrelation function (ACF) and photon counting distributions (PCDs) of R110 (calibration dye, panel A) and monomeric eGFP (panel B). PCD's were calculated with bin times of 50 μs (open circles) and 100 μs (closed circles). The experimental intensity fluctuations are shown on top. Residuals are plotted below each curve. Recovered parameters and criterion values are presented in Table 1.

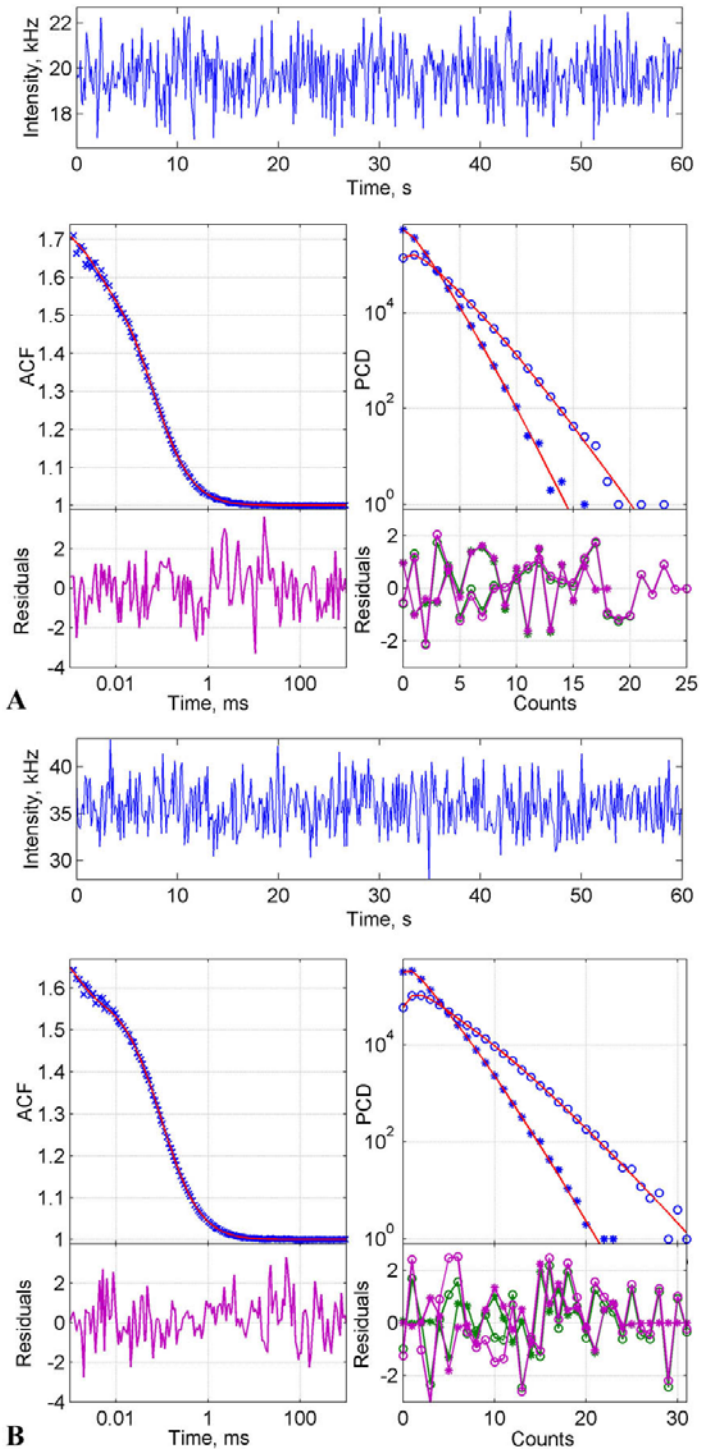

Figure 3. Results of global analysis of autocorrelation function (ACF) and photon counting distributions (PCDs) of monomeric eGFP (panel A) and dimeric eGFP (panel B). PCD's were calculated with bin times of 50 µs (closed circles) and 100 µs (open circles). The experimental intensity fluctuations are shown on top. Residuals are plotted below each curve. Photon counting histogram analysis was performed with either a Gaussian or a polynomial profile. This is only indicated in the residual plots (green points: polynomial, magenta points: Gaussian), as the theoretical curves are indistinguishable. Recovered parameters and criterion values are presented in Table 2.

Table 2. Results of global analysis of autocorrelation function (ACF) and photon counting distributions (PCDs) of monomeric eGFP and dimeric eGFP

Parameter groups	eGFP monomer PCH polynomial	eGFP monomer PCH Gaussian	eGFP dimer PCH polynomial	eGFP dimer PCH Gaussian
F_1/a_1	-0.57 ± 0.05	0.56 ± 0.03	-0.53 ± 0.02	0.65 ± 0.01
F_2/a_2	0.152 ± 0.005	0.025 ± 0.008	0.16 ± 0.001	0.035 ± 0.003
a	5.0 (fixed)	5.0 (fixed)	5.0 (fixed)	5.0 (fixed)
F_{trip}	0.18 ± 0.02	0.18 ± 0.02	0.20 ± 0.03	0.19 ± 0.03
τ_{trip}, μs	2.98 ± 0.48	2.98 ± 0.49	1.27 ± 0.21	1.35 ± 0.23
τ_{diff}, μs	62.4 ± 0.47	62.4 ± 0.47	95.1 ± 0.41	95.2 ± 0.44
N_{0eff}	1.611 ± 0.007	1.611 ± 0.007	1.698 ± 0.004	1.70 ± 0.003
$q_{0C} \times 10^3$, cpsm	12.2 ± 0.6	52.33 ± 0.75	20.98 ± 0.04	94.33 ± 0.55
$q_0 \times 10^3$, cpsm	34.48	34.49	59.34	59.32
χ^2_{gl}	1.355	1.366	1.162	1.302
$\chi^2_{gl\ mod}$	1.645	1.690	1.225	1.648

PCD's were calculated with bin times of 50 μs and 100 μs. Results of PCH analysis with either a Gaussian or a polynomial profile are presented for comparison. The data consisted of 2.4×10^5 photons for eGFP-monomer and 6.5×10^5 photons for eGFP-dimer. Both χ^2 global criteria, standard and modified, are presented for comparison.

Table 3. Analysis results of eGFP monomer (measured on the first day, see Table 1) using FIMDA and PCMH approaches

Parameter	FIMDA	PCMH
F_1	0.67 ± 0.013	0.67 (fixed)
F_2	0.05 ± 0.003	0.05 (fixed)
a	6.0 (fixed)	6.0 (fixed)
F_{trip}	0.63 ± (> 100%)	0.95 ± (> 100%)
τ_{trip}, μs	0.49 ± (> 100%)	0.04 ± (> 100%)
τ_{diff}, μs	70.9 ± 0.97	70.6 ± 0.75
N_{0eff}	2.174 ± 0.019	2.168 ± 0.014
$q_{0C} \times 10^3$, cpsm	34.45 ± 0.34	34.57 ± 0.22
$q_0 \times 10^3$, cpsm	21.63	21.70
χ^2	0.991 (global)	0.603 (fit of $q(T)$, $N(T)$); 1.10 (average from sequential PCH analysis)

Bin times of PCD's were spaced from 10 μs till 3.6 ms. A quasi-logarithmic time scale was used: the bin time increment was 2^n μs ($n\geq2$), the number of successive PCDs with given increment was 4, then n was increased by 1 and the process repeated until a bin time 3.6 ms was reached. A Gaussian profile with second order correction was used in both approaches. The correction parameters F_1, F_2 in the sequential PCMH analysis were fixed to values obtained in the global analysis of PCDs (FIMDA approach). The brightness was recalculated to its true value q_0 using Eq. 20.

$D_{\text{dimer}} / D_{\text{monomer}} = (M_{\text{monomer}} / M_{\text{dimer}})^{1/3} = (1/2)^{1/3} = 0.794$.

This value is much higher than the obtained value of 0.656 and we conclude that the translational diffusion is not that for spherical (globular) proteins. When the power of 1/3 is replaced by a power of 1/2, we obtain the ratio of diffusion constants for rod-like macromolecules and the value is 0.707, which is closer to the experimental value of 0.656. eGFP-monomer and eGFP-dimer move like rod-like molecules, which is in excellent agreement with the results of recent FCS experiments on eGFP oligomers (77).

6. CONCLUSIONS

We have presented the theory of global analysis of autocorrelation functions and photon counting distributions. Although the theories of FCS and PCH are well known, several important points have to be taken into consideration when both theories are combined in a global analysis. From the PCH side there are two major points. First, a correction must be applied for out-of-focus emission, which can be done by either a correction of the Gaussian profile via Eq. 12, or using a polynomial profile. Second, PCH must be corrected for dynamic processes allowing time-independent estimation of brightness values and number of molecules. From the FCS side the correction on difference in brightness values must be applied when multiple fluorescent species are present. The last important point is to use the same reference volume in both FCS and PCH. The use of the effective volume V_{eff} is preferable, because it allows linking the number of molecules (N) through all FCS, PCH and FIDA models.

We have described a global analysis protocol that simultaneously recovers the relevant parameters in model functions of FCS and PCH from a single fluorescence fluctuation trace allowing the linking of common parameters. The analysis yields more accurate values of triplet-state and diffusion parameters, but also robust, time-independent estimations of molecular brightness and number of molecules. We have used a new data analysis software, the FFS data processor, which allows complete analysis of experimental fluorescence fluctuation data. The use of the software is demonstrated through fitting of experimental data obtained from monomeric and dimeric forms of eGFP in aqueous buffer. Information on this software is available at www.sstcenter.com.

7. REFERENCES

1. D. Magde, E. Elson and W. W. Webb: Thermodynamic fluctuations in a reaction system: Measurement by fluorescence correlation spectroscopy. *Phys. Rev. Letters*, 29(11), 705-708 (1972)

2. E. L. Elson and D. Magde: Fluorescence correlation spectroscopy. I Conceptual basis and theory. *Biopolymers*, 13, 1-27 (1974)

3. D. Magde, E. L. Elson and W. W. Webb: Fluorescence correlation spectroscopy. II. An experimental realization. *Biopolymers*, 13(1), 29-61 (1974)

4. N. L. Thompson: Fluorescence correlation spectroscopy. In: *Topics in Fluorescence Spectroscopy*. Ed J. R. Lakowicz. Plenum Press, New York, Vol. 1, 337-378 (1991)

5. R. Rigler, U. Mets, J. Widengren and P. Kask: Fluorescence correlation spectroscopy with high count rate and low background: Analysis of translational diffusion. *Eur. Biophys. J.*, 22, 169-175 (1993)

6. M. Eigen and R. Rigler: Sorting single molecules: application to diagnostics and evolutionary biotechnology. *Proc Natl Acad Sci U S A*, 91(13), 5740-7 (1994)

7. K. M. Berland, P. T. So and E. Gratton: Two-photon fluorescence correlation spectroscopy: method and application to the intracellular environment. *Biophys J*, 68(2), 694-701 (1995)

8. K. M. Berland, P. T. So, Y. Chen, W. W. Mantulin and E. Gratton: Scanning two-photon fluctuation correlation spectroscopy: particle counting measurements for detection of molecular aggregation. *Biophys J*, 71(1), 410-20 (1996)

9. K. M. Berland: Fluorescence correlation spectroscopy: New methods for detecting molecular associations. *Biophys. J.*, 72(4), 1487-1488 (1997)

10. S. Maiti, U. Haupts and W. W. Webb: Fluorescence correlation spectroscopy: diagnostics for sparse molecules. *Proc Natl Acad Sci U S A*, 94(22), 11753-7 (1997)

11. N. L. Thompson, A. M. Lieto and N. W. Allen: Recent advances in fluorescence correlation spectroscopy. *Curr. Opin. Struct. Biol.*, 12(5), 634-41 (2002)

12. K. Bacia, S. A. Kim and P. Schwille: Fluorescence cross-correlation spectroscopy in living cells. *Nature Methods*, 3(2), 83-89 (2006)

13. E. Haustein and P. Schwille: Fluorescence correlation spectroscopy: Novel variations of an established technique. *Annu. Rev. Biophys. Biomol. Struct.*, 36, 151-169 (2007)

14. W. Al-Soufi, B. Reija , S. Felekyan, C. A. M. Seidel and M. Novo: Dynamics of supramolecular association monitored by fluorescence correlation spectroscopy. *ChemPhysChem*, 9(13), 1819-1827 (2008)

15. R. Rigler and E. S. Elson (Eds.): Fluorescence Correlation Spectroscopy. Theory and Applications. Springer, Berlin (2001)

16. S. T. Hess, S. Huang, A. A. Heikal and W. W. Webb: Biological and chemical applications of fluorescence correlation spectroscopy: a review. *Biochemistry*, 41(3), 697-705 (2002)

17. O. Krichevsky and G. Bonnet: Fluorescence correlation spectroscopy: the technique and its applications. *Rep. Prog. Phys.*, 65, 251-297 (2002)

18. Y. Chen, J. D. Müller, P. T. So and E. Gratton: The photon counting histogram in fluorescence fluctuation spectroscopy. *Biophys J*, 77(1), 553-67 (1999)

19. Y. Chen, J. D. Müller, S. Y. Tetin, J. D. Tyner and E. Gratton: Probing ligand protein binding equilibria with fluorescence fluctuation spectroscopy. *Biophys J*, 79(2), 1074-84 (2000)

20. J. D. Müller, Y. Chen and E. Gratton: Resolving heterogeneity on the single molecular level with the photon-counting histogram. *Biophys J*, 78(1), 474-86 (2000)

21. Y. Chen, J. D. Müller, Q. Ruan and E. Gratton: Molecular brightness characterization of eGFP *in vivo* by fluorescence fluctuation spectroscopy. *Biophys. J.*, 82, 133-144 (2002)

22. Y. Chen, L.-N. Wei and J. D. Müller: Probing protein oligomerization in living cells with fluorescence fluctuation spectroscopy. *Proc. Natl. Acad. Sci. USA*, 100(26), 15492-15497 (2003)

23. P. Kask, K. Palo, D. Ullmann and K. Gall: Fluorescence-intensity distribution analysis and its application in biomolecular detection technology. *Proc. Natl. Acad. Sci. USA*, 96(24), 13756-13761 (1999)

24. P. Kask, K. Palo, N. Fay, L. Brand, U. Mets, D. Ullmann, J. Jungmann, J. Pschorr and K. Gall: Two-dimensional fluorescence intensity distribution analysis: Theory and applications. *Biophys. J.*, 78(4), 1703-1713 (2000)

25. K. Palo, U. Metz, S. Jager, P. Kask and K. Gall: Fluorescence intensity multiple distributions analysis: Concurrent determination of diffusion times and molecular brightness. *Biophys. J.*, 79(6), 2858-2866 (2000)

26. K. Palo, U. Mets, V. Loorits and P. Kask: Calculation of photon count number distributions via master equations. *Biophys. J.*, 90, 2179-2191 (2006)

27. F. Meng and H. Ma: A comparison between photon counting histogram and fluorescence intensity distribution analysis. *J. Phys. Chem. B*, 110(51), 25716-25720 (2006)

28. T. Kogure, S. Karasawa, T. Araki, K. Saito, M. Kinjo and A. Miyawaki: A fluorescent variant of a protein from the stony coral Montipora facilitates dual-color single-laser fluorescence cross-correlation spectroscopy. *Nat Biotechnol*, 24(5), 577-81 (2006)

29. P. Liu, T. Sudhaharan, R. M. Koh, L. C. Hwang, S. Ahmed, I. N. Maruyama and T. Wohland: Investigation of

the dimerization of proteins from the epidermal growth factor receptor family by single wavelength fluorescence cross-correlation spectroscopy. *Biophys J*, 93(2), 684-98 (2007)

30. T. Rosales, V. Georget, D. Malide, A. Smirnov, J. Xu, C. Combs, J. R. Knutson, J. C. Nicolas and C. A. Royer: Quantitative detection of the ligand-dependent interaction between the androgen receptor and the co-activator, Tif2, in live cells using two color, two photon fluorescence cross-correlation spectroscopy. *Eur. Biophys. J.*, 36, 153-161 (2007)

31. M. A. Hink, K. Shah, E. Russinova, S. C. de Vries and A. J. W. G. Visser: Fluorescence fluctuation analysis of *Arabidopsis thaliana* somatic embryogenesis receptor-like kinase and brassinosteroid insensitive 1 receptor oligomerization. *Biophys. J.*, 94(3), 1052-1062 (2008)

32. G. Vamosi, N. Baudendistel, C. W. von der Lieth, N. Szaloki, G. Mocsar, G. Muller, P. Brazda, W. Waldeck, S. Damjanovich, J. Langowski and K. Toth: Conformation of the c-Fos/c-Jun complex *in vivo*: a combined FRET, FCCS, and MD-modeling study. *Biophys J*, 94(7), 2859-68 (2008)

33. S. Zorrilla, A. Ortega, D. Chaix, C. Alfonso, G. Rivas, S. Aymerich, M. P. Lillo, N. Declerck and C. A. Royer: Characterization of the control catabolite protein of gluconeogenic genes repressor by fluorescence cross-correlation spectroscopy and other biophysical approaches. *Biophys J*, 95(9), 4403-15 (2008)

34. T. Sudhaharan, P. Liu, Y. H. Foo, W. Bu, K. B. Lim, T. Wohland and S. Ahmed: Determination of *in vivo* dissociation constant, KD, of Cdc42-effector complexes in live mammalian cells using single wavelength fluorescence cross-correlation spectroscopy. *J Biol Chem*, 284(20), 13602-9 (2009)

35. Y. Chen, M. Tekmen, L. Hillesheim, J. Skinner, B. Wu and J. D. Müller: Dual-color photon-counting histogram. *Biophys. J.*, 88(3), 2177-2192 (2005)

36. Y. Chen and J. D. Müller: Determining the stoichiometry of protein heterocomplexes in living cells with fluorescence fluctuation spectroscopy. *Proc Natl Acad Sci U S A*, 104(9), 3147-52 (2007)

37. T. Dertinger, V. Pacheco, I. von der Hocht, R. Hartmann, I. Gregor and J. Enderlein: Two-focus fluorescence correlation spectroscopy: a new tool for accurate and absolute diffusion measurements. *ChemPhysChem*, 8(3), 433-43 (2007)

38. Y. Korlann, T. Dertinger, X. Michalet, S. Weiss and J. Enderlein: Measuring diffusion with polarization-modulation dual-focus fluorescence correlation spectroscopy. *Opt Express*, 16(19), 14609-16 (2008)

39. A. Loman, T. Dertinger, F. Koberling and J. Enderlein: Comparison of optical saturation effects in conventional and dual-focus fluorescence correlation spectroscopy. *Chem. Phys. Lett.*, 459(1-6), 18-21 (2008)

40. A. N. Kapanidis, N. K. Lee, T. A. Laurence, S. Doose, E. Margeat and S. Weiss: Fluorescence-aided molecule sorting: analysis of structure and interactions by alternating-laser excitation of single molecules. *Proc Natl Acad Sci U S A*, 101(24), 8936-41 (2004)

41. B. K. Müller, E. Zaychikov, C. Brauchle and D. C. Lamb: Pulsed interleaved excitation. *Biophys J*, 89(5), 3508-22 (2005)

42. G. Persson, P. Thyberg and J. Widengren: Modulated fluorescence correlation spectroscopy with complete time range information. *Biophys J*, 94(3), 977-85 (2008)

43. A. Benda, V. Fagul'ova, A. Deyneka, J. Enderlein and M. Hof: Fluorescence lifetime correlation spectroscopy combined with lifetime tuning: new perspectives in supported phospholipid bilayer research. *Langmuir*, 22(23), 9580-5 (2006)

44. J. Humpolickova, A. Benda, J. Sykora, R. Machan, T. Kral, B. Gasinska, J. Enderlein and M. Hof: Equilibrium dynamics of spermine-induced plasmid DNA condensation revealed by fluorescence lifetime correlation spectroscopy. *Biophys J*, 94(3), L17-9 (2008)

45. Z. Petrasek and P. Schwille: Precise measurement of diffusion coefficients using scanning fluorescence correlation spectroscopy. *Biophys J*, 94(4), 1437-48 (2008)

46. A. M. Lieto and N. L. Thompson: Total internal reflection with fluorescence correlation spectroscopy: Nonfluorescent competitors. *Biophys. J.*, 87(2), 1268-1278 (2004)

47. K. Hassler, T. Anhut, R. Rigler, M. Gosch and T. Lasser: High count rates with total internal reflection fluorescence correlation spectroscopy. *Biophys J*, 88(1), L01-3 (2005)

48. Y. Ohsugi, K. Saito, M. Tamura and M. Kinjo: Lateral mobility of membrane-binding proteins in living cells measured by total internal reflection fluorescence correlation spectroscopy. *Biophys J*, 91(9), 3456-64 (2006)

49. N. L. Thompson and B. L. Steele: Total internal reflection with fluorescence correlation spectroscopy. *Nat. Protocols*, 2(4), 878-90 (2007)

50. D. L. Kolin and P. W. Wiseman: Advances in image correlation spectroscopy: Measuring number densities, aggregation states, and dynamics of fluorescently labeled macromolecules in cells. *Cell Biochem. Biophys.*, 49(3), 141-164 (2007)

51. M. A. Digman, C. M. Brown, P. Sengupta, P. W. Wiseman, A. R. Horwitz and E. Gratton: Measuring fast dynamics in solutions and cells with a laser scanning microscope. *Biophys. J.*, 89, 1317-1327 (2005)

52. M. A. Digman, P. Sengupta, P. W. Wiseman, C. M. Brown, A. R. Horwitz and E. Gratton: Fluctuation correlation spectroscopy with a laser-scanning microscope: exploiting the hidden time structure *Biophys. J.*, 89, L33-L36 (2005)

53. M. A. Digman, P. W. Wiseman, A. R. Horwitz and E. Gratton: Detecting protein complexes in living cells from laser scanning confocal image sequences by the cross correlation raster image spectroscopy method. *Biophys J*, 96(2), 707-16 (2009)

54. S. T. Hess and W. W. Webb: Focal volume optics and experimental artifacts in confocal fluorescence correlation spectroscopy. *Biophys. J.*, 83(4), 2300-2317 (2002)

55. L. N. Hillesheim and J. D. Müller: The photon counting histogram in fluorescence fluctuation spectroscopy with non-ideal photodetectors. *Biophys. J.*, 85(3), 1948-1958 (2003)

56. J. Enderlein, I. Gregor, D. Patra, T. Dertinger and U. B. Kaupp: Performance of fluorescence correlation spectroscopy for measuring diffusion and concentration. *ChemPhysChem*, 6(11), 2324-36 (2005)

57. I. Gregor, D. Patra and J. Enderlein: Optical saturation in fluorescence correlation spectroscopy under continuous-wave and pulsed excitation. *ChemPhysChem*, 6(1), 164-70 (2005)

58. T. D. Perroud, B. Huang, M. I. Wallace and R. N. Zare: Photon counting histogram for one-photon excitation. *ChemPhysChem*, 4(10), 1121-1123 (2003)

59. B. Huang, T. D. Perroud and R. N. Zare: Photon counting histogram: One-photon excitation. *ChemPhysChem*, 5, 1523-1531 (2004)

60. T. D. Perroud, B. Huang and R. N. Zare: Effect of bin time on the photon counting histogram for one-photon excitation. *ChemPhysChem*, 6(5), 905-912 (2005)

61. V. V. Skakun, M. A. Hink, A. V. Digris, R. Engel, E. G. Novikov, V. V. Apanasovich and A. J. Visser: Global analysis of fluorescence fluctuation data. *Eur Biophys J*, 34(4), 323-34 (2005)

62. J. D. Müller. Cumulant analysis in fluctuation spectroscopy. *Biophys J*, 86, 3981-3992 (2004)

63. I. Shingaryov, V. V. Skakun and V. V. Apanasovich: Photon counts simulation in fluorescence fluctuation spectroscopy. In: *Pattern Recognition and Information Processing*. Eds. V. Krasnoproshin *et al.*, Publ. center of BSU, Minsk, 178-182 (2009)

64. I. V. Gopich and A. Szabo: Photon counting histograms for diffusive fluorophores. *J. Phys. Chem. B*, 109, 17683-17688 (2005)

65. E. Novikov and N. Boens: Analytical model of the fluorescence fluctuation spectroscopy experiment. *J. Chem. Phys.*, 114, 1745-1753 (2001)

66. P. R. Bevington and D. K. Robinson: Data Reduction and Error Analysis for the Physical Sciences. McGraw-Hill, New York (2003)

67. T. Wohland, R. Rigler and H. Vogel: The standard deviation in fluorescence correlation spectroscopy. *Biophys. J.*, 80, 2987-2999 (2001)

68. A. J. W. G. Visser, S. P. Laptenok, N. V. Visser, A. van Hoek, D. J. S. Birch, J. C. Brochon and J. W. Borst: Time-resolved FRET fluorescence spectroscopy of visible fluorescent protein pairs. *Eur. Biophys. J.*, 39, 241-253 (2010)

69. M. A. Hink, J. W. Borst and A. J. W. G. Visser: Fluorescence correlation spectroscopy of GFP fusion proteins in living plant cells. *Methods Enzymol.*, 361, 93-112 (2003)

70. K. Weisshart, V. Jüngel and S. J. Briddon: The LSM 510 META - ConfoCor 2 system: An integrated imaging and spectroscopic platform for single-molecule detection. *Curr. Pharm. Biotechnol.*, 5, 135-154 (2004)

71. J. Widengren, U. Mets and R. Rigler: Fluorescence correlation spectroscopy of triplet states in solution: A theoretical and experimental study. *J. Phys. Chem.*, 99, 13368-13379 (1995)

72. J. M. Beechem, E. Gratton, M. Ameloot, J. R. Knutson and L. Brand: Analysis of fluorescence intensity and anisotropy decay data: Second generation theory and programs. In: *Topics in Fluorescence Spectroscopy.* Ed. J. R. Lakowicz. Plenum Press, New York, Vol. 2, 241- 305 (1991)

73. M. L. Johnson and L. M. Faunt: Parameter estimation by least-squares methods. *Methods Enzymol.*, 210, 1-37 (1992)

74. V.V. Skakun, E.G. Novikov, V.V. Apanasovich, H.J. Tanke, A.M. Deelder, O.A. Mayboroda: Initial Guesses Generation for Fluorescence Intensity Distribution Analysis. *Eur. Biophys. J.* 35(5), 410-423 (2006)

75. H.T. Lau: A Numerical Library in C for Scientists and Engineers. CRC Press, Boca Raton (1995)

76. W.H. Press, S.A. Teukolsky, W.T. Vetterling, B.P. Flannery: Numerical Recipes in C. The art of scientific computing. 2nd ed. Cambridge University Press, Cambridge (1992)

77. N. Dross, C. Spriet, M. Zwerger, G. Muller, W. Waldeck and J. Langowski: Mapping eGFP oligomer mobility in living cell nuclei. *PLoS One*, 4(4), e5041 (2009)

Key Words: Fluorescence Fluctuation Spectroscopy, Fluorescence Correlation Spectroscopy, Photon Counting

Histogram, Fluorescence Intensity Distribution Analysis, Global Analysis, Green Fluorescent Protein

Send correspondence to: Victor V. Skakun, Department of Systems Analysis, Radio Physics and Electronics Faculty, Belarusian State University, Minsk, 220050, Belarus, Tel: 37517 2789665, Fax: 37517 2789345, E-mail: skakun@sstcenter.com

http://www.bioscience.org/current/vol3E.htm